Available online at www.sciencedirect.com
SCIENCE DIRECT®
ELSEVIER
International Journal of Solids and Structures 43 (2006) 2336–2350
INTERNATIONAL JOURNAL OF SOLIDS and STRUCTURES
www.elsevier.com/locate/ijsolstr

Piezoelectric study on circularly cylindrical layered media

M.H. Shen *, F.M. Chen, S.N. Chen

Department of Mechanical Engineering, Nan Kai Institute of Technology, 568 Chung Cheng Road, Tsao Tun, 542 Nantou County, Taiwan

Received 4 January 2005; received in revised form 1 May 2005
Available online 1 July 2005

Abstract

In this paper, an analytical solution in series form for the problem of a circularly cylindrical layered piezoelectric composite consisting of N dissimilar layers is presented within the framework of linear piezoelectricity. Each layer of the composite is assumed to be transversely isotropic with respect to the longitudinal direction (x_3 direction), and the composite is subject to arbitrary electromechanical singularities infinitely extended in a direction perpendicular to the x_1–x_2 plane such that only in-plane electric fields and out-of-plane displacement are produced. The alternating technique in conjunction with the method of analytical continuation is applied to derive the general multilayered media solution in an explicit series form, whose convergence is guaranteed numerically. The distributions of the shear stress and electric field are found to be dependent on the material combinations and the magnitude and position of the electromechanical singularities. An exactly closed form solution is obtained and discussed graphically for a practical example.

Keywords: Circularly cylindrical layered piezoelectric media; Alternating technique; Electromechanical loading

1. Introduction

The development of piezoelectric materials or structures has been made by the research community in recent years. It is well known that piezoelectric materials produce an electric field when deformed, and undergo deformation when subjected to an electric field. The electromechanical coupling effect of piezoelectric materials plays a significant role in many modern devices and composite structures, such as electromechanical transducers, thermal sensors, electronic packaging, and micro power generator. When subjected to mechanical and electrical loads in service, these piezoelectric materials can fail prematurely due to defects

* Corresponding author. Tel.: +886 495634893412; fax: +886 49565674.
E-mail address: mhshen@nkc.edu.tw (M.H. Shen).

0020-7683/$ - see front matter © 2005 Elsevier Ltd. All rights reserved.
doi:10.1016/j.ijsolstr.2005.05.010

during their manufacturing process. Therefore, it is important to analyze the behavior of various defects such as cracks, dislocations and inclusions in electrical and mechanical fields that predict the performance and integrity of these devices. Indeed, a number of contributions concerning the defective problem in piezoelectric materials have appeared in the literature. These include the work of (Pak, 1992; Honein et al., 1995; Zhong and Meguid, 1997; Weichen, 1997; Meguid and Deng, 1998; Deng and Meguid, 1999; Liu et al., 2000; Lee et al., 2000; Wang and Shen, 2001; Huang and Kuang, 2001), among others. However, such existing studies are only limited to bimaterial problems or two-phase models of inclusion/matrix. Based on the complex variable theory in conjunction with the Möebius transformation, Chao and Chang (1999) studied the problem of multiple piezoelectric circular inclusions embedded in an infinite matrix. Jiang and Cheung (2001) proposed a three-phase piezoelectric cylinder model and gave an exact solution by using the Laurent expansion technique, but their result is based on a uniform far-field loading condition. Liu et al. (2004) developed a method that dealt with the interaction of a piezoelectric screw dislocation with an interphase layer between the circular inclusion and the piezoelectric matrix. To our knowledge, the electro-elastic behavior of multiplying connected region with more than three different material subjected to mechanical and electric loadings has not been recorded in the literature. It is therefore the purpose of the current paper to provide a theoretical treatment for the problem of circularly cylindrical layered media in anti-plane piezoelectricity. The developed model can be applied to a variety of problems, for example, a finite multiple phase cylinder and a bimaterial concentric annulus etc. The composite is subjected to arbitrary loadings including a point force and point charge. The proposed method is based on the technique of analytical continuation that is alternatively applied across all concentric interfaces in order to derive the solution of the composite in a series form from the corresponding homogeneous solution. This method has a clear advantage in deriving the solution to the heterogeneous problem in terms of the solution to the corresponding homogeneous problem that was termed "heterogenization" by Honein et al. (1992a,b).

This paper is divided into six sections. Following this brief introduction, a complex representation of anti-plane piezoelectricity is provided in Section 2, and the solutions of a singularity problem of a bimaterial and a multiplying connected region are provided in Sections 3and 4, respectively. In Section 5, some numerical results are presented graphically to show the distribution of normal shear stress and electric field for different material constant combinations. Finally, a conclusion is made for the current article in Section 6.

2. A complex representation of anti-plane piezoelectricity

Consider a piezoelectric composite composed of any number of dissimilar materials bonded along concentric circular interfaces. Each layer is assumed to have the same material orientation with x_3 in the poling direction. In a class of piezoelectric materials capable of undergoing out-of-plane displacement u_3 and in-plane electric potential ϕ, it is convenient to use a complex representation for u_3 and ϕ which are grouped as a vector

$$\mathrm{Re}[\mathbf{U}] = \begin{Bmatrix} u_3 \\ \phi \end{Bmatrix} \tag{1}$$

where Re denotes the real part of a complex function and $\mathbf{U}$ is the generalized displacement with two components being holomorphic functions. The components of the stress and electric displacement are related to the generalized displacement by

$$\begin{Bmatrix} \sigma_{31} - \mathrm{i}\sigma_{32} \\ D_1 - \mathrm{i}D_2 \end{Bmatrix} = \begin{bmatrix} c_{44} & e_{15} \\ e_{15} & -\varepsilon_{11} \end{bmatrix} \mathbf{U}' = \mathbf{C}\mathbf{U}' \tag{2}$$

where prime indicates differentiation with respect to the complex variable $z = x_1 + ix_2$. In order to express the boundary condition in terms of $\mathbf{U}$ rather than its derivative $\mathbf{U}'$, we take an integration of the traction t and normal electric displacement D_n as

$$\int \begin{Bmatrix} t \\ D_n \end{Bmatrix} \mathrm{d}s = \mathrm{Im}[\mathbf{CU}] \tag{3}$$

where $[t\, D_n]^{\mathrm{T}}$ is referred to as the generalized traction and Im denotes the imaginary part of a complex function.

3. Solution for a single inclusion problem

Consider a circular piezoelectric inclusion bonded along the circular interface $r = a$ with a singularity located in the outer region (see Fig. 1). Where S_a, the inner region, and S_b, the outer region, are occupied by material a and b, respectively. By applying the continuity conditions of Re[$\mathbf{U}$] and Im[$\mathbf{CU}$] along the interface, and using the method of analytical continuation, one can obtain the solution for the current problem as

$$\mathbf{U}(z) = \begin{cases} \boldsymbol{\alpha}_{ab}\mathbf{U}(z) & z \in S_a \\ \mathbf{U}(z) + \boldsymbol{\beta}_{ab}\overline{\mathbf{U}}\left(\frac{a^2}{z}\right) & z \in S_b \end{cases} \tag{4}$$

where

$$\boldsymbol{\alpha}_{ab} = 2(\mathbf{C}_a + \mathbf{C}_b)^{-1}\mathbf{C}_b$$

$$\boldsymbol{\beta}_{ab} = (\mathbf{C}_a + \mathbf{C}_b)^{-1}(\mathbf{C}_b - \mathbf{C}_a)$$

$$\mathbf{C}_a = \begin{bmatrix} c_{44}^a & e_{15}^a \\ e_{15}^a & -\varepsilon_{11}^a \end{bmatrix}$$

$$\mathbf{C}_b = \begin{bmatrix} c_{44}^b & e_{15}^b \\ e_{15}^b & -\varepsilon_{11}^b \end{bmatrix}$$

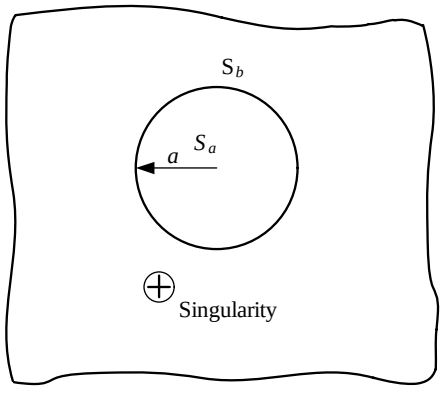

Fig. 1. A circular inclusion embedded in an infinite matrix.

and $\mathbf{U}(z)$ represents the solution corresponding to the homogeneous medium which is holomorphic in the entire domain except for some singular points. The solution for a homogeneous infinite body subjected to a point force p_0 and a point charge q_0 can be trivially given as

$$\mathbf{U}(z) = \begin{bmatrix} \dfrac{-\varepsilon_{11}^b p_0 + e_{15}^b q_0}{c_{44}^b \varepsilon_{11} + (e_{15}^b)^2} \\ -\dfrac{e_{15}^b p_0 + c_{44}^b q_0}{c_{44}^b \varepsilon_{11} + (e_{15}^b)^2} \end{bmatrix} \log(z - z_0) = \mathbf{D}_b \log(z - z_0) \tag{5}$$

For a singularity located in the inner region, since the homogeneous solution is neither holomorphic in S_a nor holomorphic in S_b, it should be rewritten as

$$\mathbf{U}(z) = \mathbf{D}_a \log z + \mathbf{U}^*(z)$$

where $\mathbf{D}_a$ is defined as $\mathbf{D}_b$ in Eq. (5), but the piezoelectric constants involved in $\mathbf{D}_a(z)$ are for material a, and

$$\mathbf{U}^*(z) = \mathbf{D}_a \log\left(1 - \frac{z_0}{z}\right)$$

which is holomophic in the outer region S_b. By applying the continuity conditions of Re[$\mathbf{U}$] and Im[$\mathbf{CU}$] along the interface, and using the method of analytical continuation, one can obtain

$$\begin{cases} \mathbf{U}_a(z) = \mathbf{U}(z) + \boldsymbol{\beta}_{ba} \overline{\mathbf{U}}^*\left(\frac{a^2}{z}\right) & z \in S_a \\ \mathbf{U}_b(z) = \mathbf{D}_b \log\left(\frac{z}{a}\right) + \mathbf{D}_a \log(a) + \boldsymbol{\alpha}_{ba} \mathbf{U}^*(z) & z \in S_b \end{cases} \tag{6}$$

4. A singularity in a multilayered media and the alternating technique

The alternating technique together with the results of the previous section can be used to analyze a singularity in a circularly cylindrical layered media as shown in Figs. 2 and 7. Since it is difficult to satisfy the continuity conditions along all interfaces at the same time, the method of analytical continuation should be applied to all interfaces alternatively.

4.1. A multilayered media with singularities embedded in the outer region

Consider the circularly cylindrical layered media with singularities embedded in the outer region S_0 (see Fig. 2). The complex potential of each layer can be expressed as

$$\mathbf{U}_i(z) = \sum_{n=1}^{\infty} \mathbf{U}_{ia}^n(z) + \sum_{n=1}^{\infty} \mathbf{U}_{ib}^n(z) \tag{7}$$

where $\mathbf{U}_{ia}^n(z)$ and $\mathbf{U}_{ib}^n(z)$ are respectively holomorphic in region $r \leqslant r_i$ and region $r \geqslant r_i$. By applying the method of analytical continuation to all interfaces alternatively, the unknown potentials can be expressed in terms of homogenous solution $\mathbf{U}(z)$. First, we introduce two perturbed function $\mathbf{U}_{1a}^1(z)$ and $\mathbf{U}_{0b}^1(z)$ which are holomorphic in region $r \leqslant r_0$ and region $r \geqslant r_0$, respectively, to satisfy the continuous conditions of interface L_0. These two terms can be determined by the method of analytical continuation. But they cannot satisfy the continuity conditions at the other interfaces including L_1. Hence another two additional terms $\mathbf{U}_{2a}^1(z)$, $\mathbf{U}_{1b}^1(z)$ holomorphic in $r \leqslant r_1$ and $r \geqslant r_1$, respectively, are introduced and solved again to satisfy the continuity conditions across L_1. Of course, they still can not satisfy the continuous conditions of other

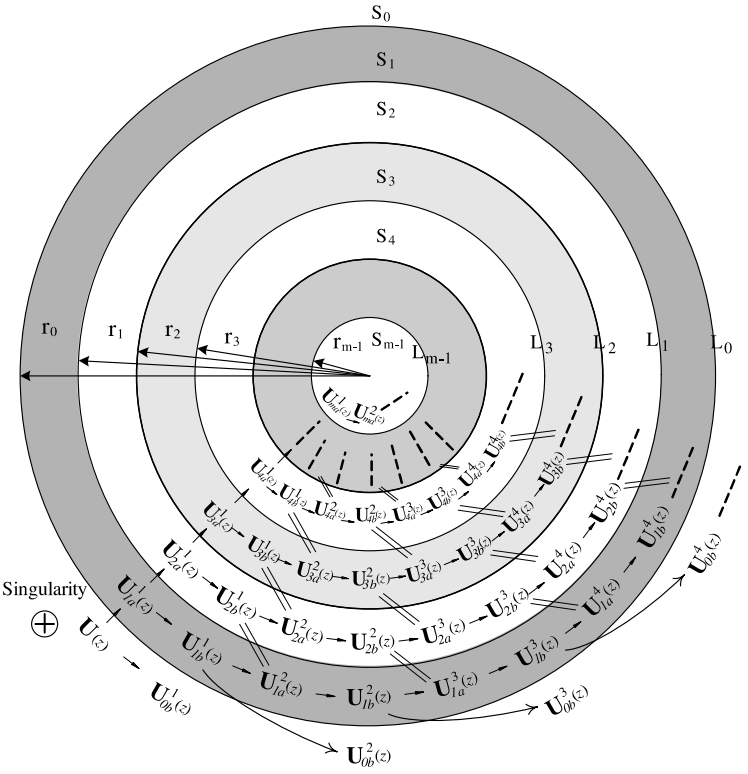

Fig. 2. Procedure for solving the problem of a multilayered media with a singularity located in the outer region.

interfaces. In order to satisfy the continuous conditions for all interfaces, the previous steps are repeated to achieve the other terms $\mathbf{U}^1_{ia}(z)$, $\mathbf{U}^1_{(i-1)b}(z)$ for $i = 3,4,\ldots,m$ and $\mathbf{U}^n_{ia}(z)$, $\mathbf{U}^n_{(i-1)b}(z)$ for $i = 1,2,3,\ldots,m$; $n = 2,3,4\ldots$ (see Fig. 2). Finally the unknown functions are obtained.

$$\begin{cases} \mathbf{U}^1_{0a}(z) = \mathbf{U}(z) \\ \mathbf{U}^n_{0a}(z) = 0 \quad n = 2,3,4,\ldots \\ \mathbf{U}^n_{mb}(z) = 0 \quad n = 1,2,3,\ldots \end{cases} \tag{8}$$

$$\begin{cases} \mathbf{U}^1_{ia}(z) = \boldsymbol{\alpha}_{i(i-1)}\mathbf{U}^1_{(i-1)a}(z) \\ \mathbf{U}^1_{(i-1)b}(z) = \boldsymbol{\beta}_{i(i-1)}\overline{\mathbf{U}}^1_{(i-1)a}\left(\frac{r^2_{i-1}}{z}\right) \end{cases} \quad \text{for } i = 1,2,3,\ldots \tag{9}$$

$$\begin{cases} \mathbf{U}^n_{ia}(z) = \boldsymbol{\alpha}_{i(i-1)}\mathbf{U}^n_{(i-1)a}(z) + \boldsymbol{\beta}_{(i-1)i}\overline{\mathbf{U}}^{n-1}_{ib}\left(\frac{r^2_{i-1}}{z}\right) \\ \mathbf{U}^n_{(i-1)b}(z) = \boldsymbol{\alpha}_{(i-1)i}\mathbf{U}^{n-1}_{ib}(z) + \boldsymbol{\beta}_{i(i-1)}\overline{\mathbf{U}}^n_{(i-1)a}\left(\frac{r^2_{i-1}}{z}\right) \end{cases} \quad \text{for } i = 1,2,3,\ldots;\ n = 2,3,4,\ldots \tag{10}$$

4.1.1. A four-layer composite

For the case of four-layer composite with singularities located in the outer region S_0 (Fig. 3), by the same procedures used in the previous section, the solution can be obtained as

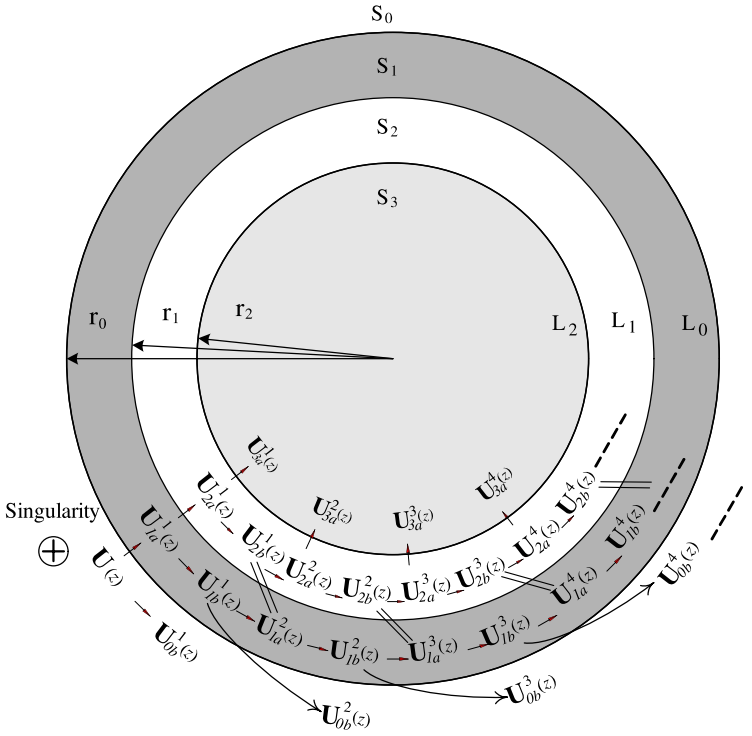

Fig. 3. Procedure for solving the problem of a four-layer composite with a singularity located in the outer region.

$$\begin{cases} \mathbf{U}_0(z) = \mathbf{U}(z) + \sum_{n=1}^{\infty} \mathbf{U}_{0b}^n(z) \\ \mathbf{U}_1(z) = \sum_{n=1}^{\infty} \mathbf{U}_{1a}^n(z) + \sum_{n=1}^{\infty} \mathbf{U}_{1b}^n(z) \\ \mathbf{U}_2(z) = \sum_{n=1}^{\infty} \mathbf{U}_{2a}^n(z) + \sum_{n=1}^{\infty} \mathbf{U}_{2b}^n(z) \\ \mathbf{U}_3(z) = \sum_{n=1}^{\infty} \mathbf{U}_{3a}^n(z) \end{cases} \tag{11}$$

where

$$\mathbf{U}_{1a}^1(z) = \boldsymbol{\alpha}_{10}\mathbf{U}(z)$$
$$\mathbf{U}_{2a}^1(z) = \boldsymbol{\alpha}_{21}\boldsymbol{\alpha}_{10}\mathbf{U}(z)$$
$$\mathbf{U}_{3a}^1(z) = \boldsymbol{\alpha}_{32}\boldsymbol{\alpha}_{21}\boldsymbol{\alpha}_{10}\mathbf{U}(z)$$
$$\mathbf{U}_{0b}^1(z) = \boldsymbol{\beta}_{10}\overline{\mathbf{U}}\left(\frac{r_0^2}{z}\right)$$
$$\mathbf{U}_{1b}^1(z) = \boldsymbol{\beta}_{21}\boldsymbol{\alpha}_{10}\overline{\mathbf{U}}\left(\frac{r_1^2}{z}\right)$$
$$\mathbf{U}_{2b}^1(z) = \boldsymbol{\beta}_{32}\boldsymbol{\alpha}_{21}\boldsymbol{\alpha}_{10}\overline{\mathbf{U}}\left(\frac{r_2^2}{z}\right)$$

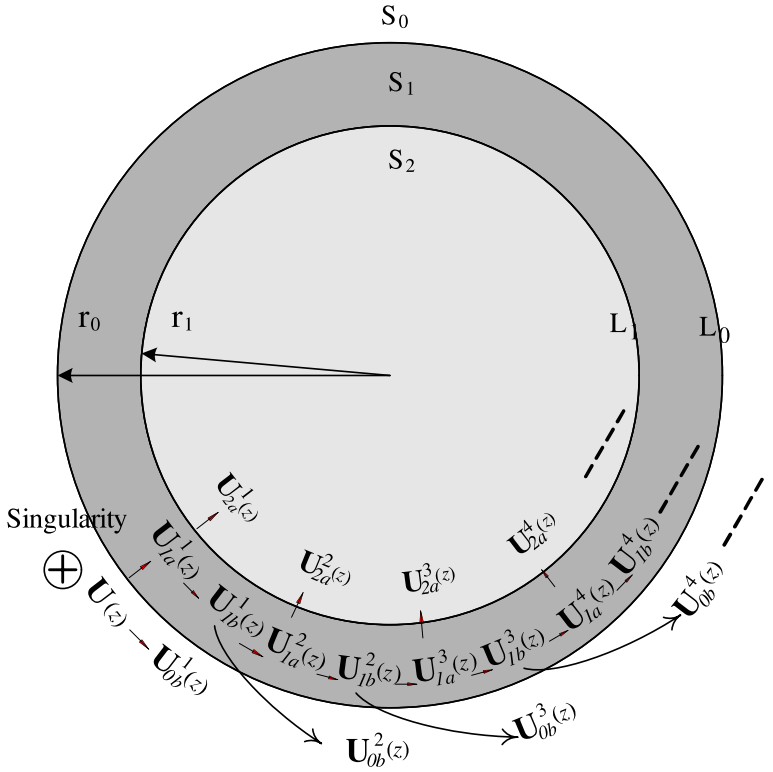

Fig. 4. Procedure for solving the problem of a three-layer composite with a singularity located in the outer region.

and

$$\mathbf{U}_{1a}^{n}(z)=\boldsymbol{\beta}_{01}\overline{\mathbf{U}}_{1b}^{n-1}\left(\frac{r_0^2}{z}\right)$$

$$\mathbf{U}_{2a}^{n}(z)=\boldsymbol{\beta}_{12}\boldsymbol{\beta}_{32}\mathbf{U}_{2a}^{n-1}\left(\frac{r_2^2}{r_1^2}z\right)+\boldsymbol{\alpha}_{21}\boldsymbol{\beta}_{01}\overline{\mathbf{U}}_{1b}^{n-1}\left(\frac{r_0^2}{z}\right)$$

$$\mathbf{U}_{3a}^{n}(z)=\boldsymbol{\alpha}_{32}\boldsymbol{\beta}_{12}\boldsymbol{\beta}_{32}\mathbf{U}_{2a}^{n-1}\left(\frac{r_2^2}{r_1^2}z\right)+\boldsymbol{\alpha}_{32}\boldsymbol{\alpha}_{21}\boldsymbol{\beta}_{01}\overline{\mathbf{U}}_{1b}^{n-1}\left(\frac{r_0^2}{z}\right)$$

$$\mathbf{U}_{0b}^{n}(z)=\boldsymbol{\alpha}_{01}\mathbf{U}_{1b}^{n-1}(z)$$

$$\mathbf{U}_{1b}^{n}(z)=\boldsymbol{\beta}_{21}\boldsymbol{\beta}_{01}\mathbf{U}_{1b}^{n-1}\left(\frac{r_0^2}{r_1^2}z\right)+\boldsymbol{\alpha}_{12}\boldsymbol{\beta}_{32}\overline{\mathbf{U}}_{2a}^{n-1}\left(\frac{r_2^2}{z}\right)$$

$$\mathbf{U}_{2b}^{n}(z)=\boldsymbol{\beta}_{32}\boldsymbol{\beta}_{12}\boldsymbol{\beta}_{32}\overline{\mathbf{U}}_{2a}^{n-1}\left(\frac{r_2^4}{r_1^2z}\right)+\boldsymbol{\beta}_{32}\boldsymbol{\alpha}_{21}\boldsymbol{\beta}_{01}\mathbf{U}_{1b}^{n-1}\left(\frac{r_0^2}{r_2^2}z\right)$$

4.1.2. A three-layer composite

For the case of three-layer composite with singularities in the outer region S_0 (see Fig. 4), by the same procedures used in the previous section, the solution can be obtained as

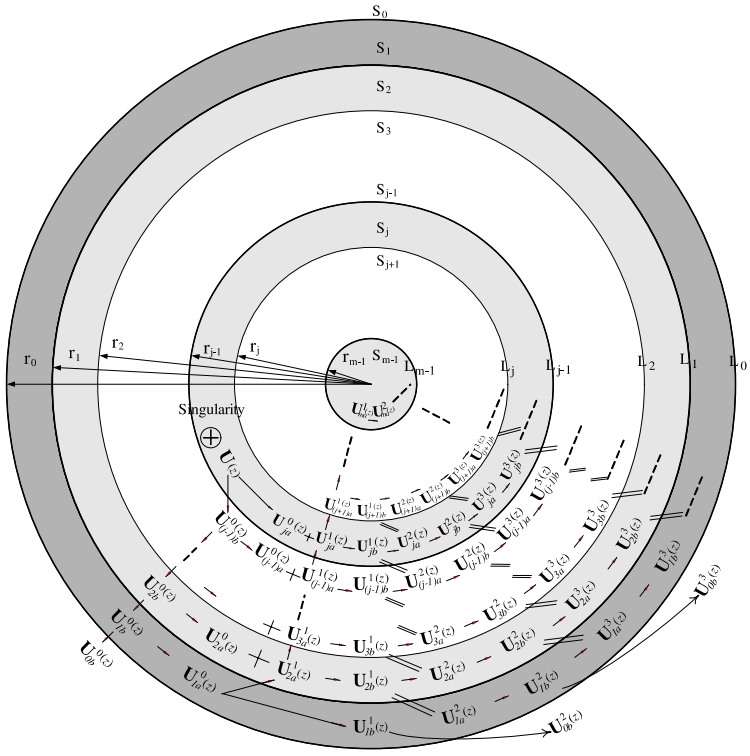

Fig. 5. Procedure for solving the problem of a multilayered media with a singularity located in the inter-layer.

$$\begin{cases} \mathbf{U}_0(z) = \mathbf{U}(z) + \boldsymbol{\beta}_{10}\overline{\mathbf{U}}\left(\frac{r_0^2}{z}\right) + \boldsymbol{\alpha}_{01}\boldsymbol{\beta}_{21}\sum_{n=0}^{\infty}(\boldsymbol{\beta}_{01}\boldsymbol{\beta}_{21})^n\boldsymbol{\alpha}_{10}\overline{\mathbf{U}}\left(\frac{r_1^{2n+2}}{r_0^{2n}}\frac{1}{z}\right) \\ \mathbf{U}_1(z) = \sum_{n=0}^{\infty}(\boldsymbol{\beta}_{01}\boldsymbol{\beta}_{21})^n\boldsymbol{\alpha}_{10}\mathbf{U}\left(\frac{r_1^{2n}}{r_0^{2n}}z\right) + \boldsymbol{\beta}_{21}\sum_{n=0}^{\infty}(\boldsymbol{\beta}_{01}\boldsymbol{\beta}_{21})^n\boldsymbol{\alpha}_{10}\overline{\mathbf{U}}\left(\frac{r_1^{2n+2}}{r_0^{2n}}\frac{1}{z}\right) \\ \mathbf{U}_2(z) = \boldsymbol{\alpha}_{21}\sum_{n=0}^{\infty}(\boldsymbol{\beta}_{01}\boldsymbol{\beta}_{21})^n\boldsymbol{\alpha}_{10}\mathbf{U}\left(\frac{r_1^{2n}}{r_0^{2n}}z\right) \end{cases} \tag{12}$$

4.2. A multilayered media with singularities embedded in the inter-layer

Consider the circularly cylindrical layered media subjected to singularities in arbitrary inter-layer S_j (see Fig. 5). The complex potential of each layer can be expressed as

$$\begin{cases} \mathbf{U}_i(z) = \mathbf{D}_i\log\left(\frac{z}{r_i}\right) + \sum_{k=i}^{j-2}\mathbf{D}_{k+1}\log\left(\frac{r_k}{r_{k+1}}\right) + \mathbf{D}_j\log(r_{j-1}) + \sum_{n=0}^{\infty}\mathbf{U}_{ia}^n(z) + \sum_{n=0}^{\infty}\mathbf{U}_{ib}^n(z) \quad \text{for } i \leqslant j-2 \\ \mathbf{U}_{j-1}(z) = \mathbf{D}_{j-1}\log\left(\frac{z}{r_{j-1}}\right) + \mathbf{D}_j\log(r_{j-1}) + \sum_{n=0}^{\infty}\mathbf{U}_{ia}^n(z) + \sum_{n=0}^{\infty}\mathbf{U}_{ib}^n(z) \\ \mathbf{U}_j(z) = \mathbf{D}_j\log(z) + \sum_{n=0}^{\infty}\mathbf{U}_{ja}^n(z) + \sum_{n=0}^{\infty}\mathbf{U}_{jb}^n(z) \\ \mathbf{U}_i(z) = \sum_{n=1}^{\infty}\mathbf{U}_{ia}^n(z) + \sum_{n=1}^{\infty}\mathbf{U}_{ib}^n(z) \quad \text{for } i > j \end{cases} \tag{13}$$

where the unknown potentials $\mathbf{U}^n_{ia}(z)$ and $\mathbf{U}^n_{ib}(z)$ are holomorphic in region $r \leqslant r_i$ and region $r \geqslant r_i$, respectively. Similarly by applying the method of analytical continuation to all interfaces alternatively, the unknown potentials can be expressed in terms of homogenous solution $\mathbf{U}(z)$ by the procedures as follows. First, we introduce two perturbed function $\mathbf{U}^0_{ja}(z)$ and $\mathbf{U}^0_{(j-1)b}(z)$ which are holomorphic in the regions $r \leqslant r_{j-1}$ and $r \geqslant r_{j-1}$, respectively, to satisfy the continuous conditions of interface L_{j-1}. Obviously, they cannot satisfy the continuity conditions of the other interfaces including L_{j-2}. In order to satisfy the continuous conditions across L_{j-2}, two additional terms $\mathbf{U}^0_{(j-1)a}(z)$, $\mathbf{U}^0_{(j-2)b}(z)$ which are holomorphic in the regions $r \leqslant r_{j-2}$ and $r \geqslant r_{j-2}$, respectively, are introduced and solved by analytical continuation method. The previous steps are repeated to achieve the other terms $\mathbf{U}^0_{ia}(z)$, $\mathbf{U}^0_{(i-1)b}(z)$ for $i = j-2, j-3, \ldots, 2, 1$. But they still cannot satisfy the continuous conditions for all interfaces simultaneously. Another terms $\mathbf{U}^1_{ia}(z)$, $\mathbf{U}^1_{(i-1)b}(z)$ for $i = 2, 3, \ldots, m$ and $\mathbf{U}^n_{ia}(z)$, $\mathbf{U}^n_{(i-1)b}(z)$ for $i = 1, 2, 3, \ldots, m$; $n = 1, 2, 3 \ldots$ as indicated in Fig. 5 must be introduced and solved. Finally the complete solution can be found to satisfy all interfacial continuous conditions and can be expressed in terms of homogeneous solution $\mathbf{U}(z)$.

$$\mathbf{U}^0_{jb}(z) = \mathbf{U}^*(z) \tag{14}$$

$$\begin{cases} \mathbf{U}^n_{0a}(z) = 0 \\ \mathbf{U}^n_{mb}(z) = 0 \end{cases} \quad \text{for } n = 1, 2, 3 \ldots \tag{15}$$

$$\begin{cases} \mathbf{U}^0_{ia}(z) = \boldsymbol{\beta}_{(i-1)i}\overline{\mathbf{U}}^0_{ib}\left(\frac{r^2_{i-1}}{z}\right) \\ \mathbf{U}^0_{(i-1)b}(z) = \boldsymbol{\alpha}_{(i-1)i}\mathbf{U}^0_{ib}(z) \end{cases} \quad \text{for } i = j, j-1, \ldots, 2, 1 \tag{16}$$

$$\begin{cases} \mathbf{U}^1_{ia}(z) = \boldsymbol{\alpha}_{i,(i-1)}\left[\mathbf{U}^0_{(i-1)a}(z) + \mathbf{U}^1_{(i-1)a}(z)\right] \quad \text{for } i = 1, 2, \ldots, j-1, j \\ \mathbf{U}^1_{(j+1)a}(z) = \boldsymbol{\alpha}_{(j+1)j}\left[\mathbf{U}(z) + \mathbf{U}^0_{ja}(z) + \mathbf{U}^1_{ja}(z)\right] \\ \mathbf{U}^1_{ia}(z) = \boldsymbol{\alpha}_{i(i-1)}\left[\mathbf{U}^1_{(i-1)a}(z)\right] \quad \text{for } i = j+2, j+1, \ldots, m-1, m \end{cases} \tag{17}$$

$$\begin{cases} \mathbf{U}^1_{ib}(z) = \boldsymbol{\beta}_{(i+1)i}\left[\mathbf{U}^0_{ia}\left(\frac{r^2_i}{z}\right) + \mathbf{U}^1_{ia}\left(\frac{r^2_i}{z}\right)\right] \quad \text{for } i = 0, 1 \ldots j-2, j-1 \\ \mathbf{U}^1_{jb}(z) = \boldsymbol{\beta}_{(j+1)j}\left[\overline{\mathbf{U}}\left(\frac{r^2_j}{z}\right) + \overline{\mathbf{U}}^0_{ja}\left(\frac{r^2_j}{z}\right) + \overline{\mathbf{U}}^1_{ja}\left(\frac{r^2_j}{z}\right)\right] \\ \mathbf{U}^1_{ib}(z) = \boldsymbol{\beta}_{(i+1)i}\left[\overline{\mathbf{U}}^1_{ia}\left(\frac{r^2_i}{z}\right)\right] \quad \text{for } i = j+1, j, \ldots, m-1, m \end{cases} \tag{18}$$

$$\begin{cases} \mathbf{U}^n_{ia}(z) = \boldsymbol{\alpha}_{i(i-1)}\mathbf{U}^n_{(i-1)a}(z) + \boldsymbol{\beta}_{(i-1)i}\overline{\mathbf{U}}^{n-1}_{ib}\left(\frac{r^2_{i-1}}{z}\right) \\ \mathbf{U}^n_{(i-1)b}(z) = \boldsymbol{\alpha}_{(i-1)i}\mathbf{U}^{n-1}_{ib}(z) + \boldsymbol{\beta}_{i(i-1)}\overline{\mathbf{U}}^n_{(i-1)a}\left(\frac{r^2_{i-1}}{z}\right) \end{cases} \quad \text{for } i = 1, 2, 3, \ldots; n = 2, 3, 4, \ldots \tag{19}$$

4.2.1. A four-layer composite

For the case of four-layer composite with a singularity located in the inter-layer S_1 (Fig. 6), by the same procedures used in the previous section, the solution can be obtained as

$$\begin{cases} \mathbf{U}_0(z) = \mathbf{D}_0 \log\left(\frac{z}{r_0}\right) + \mathbf{D}_1 \log(r_0) + \sum_{n=1}^{\infty} \mathbf{U}^n_{0b}(z) \\ \mathbf{U}_1(z) = \mathbf{U}(z) + \sum_{n=1}^{\infty} \mathbf{U}^n_{1a}(z) + \sum_{n=1}^{\infty} \mathbf{U}^n_{1b}(z) \\ \mathbf{U}_2(z) = \sum_{n=1}^{\infty} \mathbf{U}^n_{2a}(z) + \sum_{n=1}^{\infty} \mathbf{U}^n_{2b}(z) \\ \mathbf{U}_3(z) = \sum_{n=1}^{\infty} \mathbf{U}^n_{3a}(z) \end{cases} \tag{20}$$

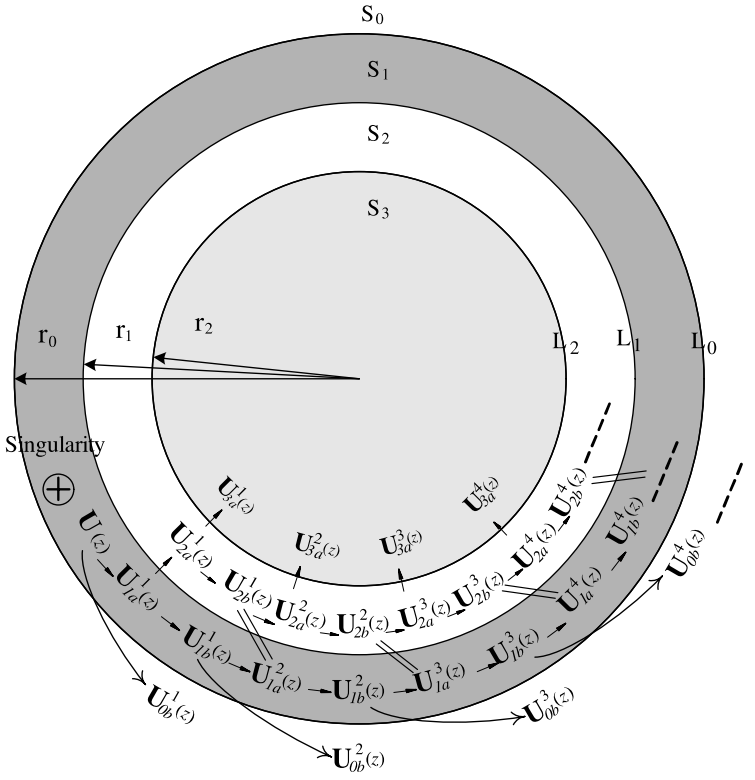

Fig. 6. Procedure for solving the problem of a four-layer composite with a singularity located in the inter-layer.

where

$$\mathbf{U}^1_{1a}(z) = \boldsymbol{\beta}_{01}\overline{\mathbf{U}^*}\left(\frac{r_0^2}{z}\right)$$

$$\mathbf{U}^1_{2a}(z) = \boldsymbol{\alpha}_{21}\left[\boldsymbol{\beta}_{01}\overline{\mathbf{U}^*}\left(\frac{r_0^2}{z}\right) + \mathbf{U}(z)\right]$$

$$\mathbf{U}^1_{3a}(z) = \boldsymbol{\alpha}_{32}\boldsymbol{\alpha}_{21}\left[\boldsymbol{\beta}_{01}\overline{\mathbf{U}^*}\left(\frac{r_0^2}{z}\right) + \mathbf{U}(z)\right]$$

$$\mathbf{U}^1_{0b}(z) = \boldsymbol{\alpha}_{01}\mathbf{U}^*(z)$$

$$\mathbf{U}^1_{1b}(z) = \boldsymbol{\beta}_{21}\left[\boldsymbol{\beta}_{01}\mathbf{U}^*\left(\frac{r_0^2}{r_1^2}z\right) + \overline{\mathbf{U}}\left(\frac{r_1^2}{z}\right)\right]$$

$$\mathbf{U}^1_{2b}(z) = \boldsymbol{\beta}_{32}\boldsymbol{\alpha}_{21}\left[\boldsymbol{\beta}_{01}\mathbf{U}^*\left(\frac{r_0^2}{r_2^2}z\right) + \overline{\mathbf{U}}\left(\frac{r_2^2}{z}\right)\right]$$

and

$$\mathbf{U}^n_{1a}(z) = \boldsymbol{\beta}_{01}\overline{\mathbf{U}}^{n-1}_{1b}\left(\frac{r_0^2}{z}\right)$$

$$\mathbf{U}^n_{2a}(z) = \boldsymbol{\beta}_{12}\boldsymbol{\beta}_{32}\mathbf{U}^{n-1}_{2a}\left(\frac{r_2^2}{r_1^2}z\right) + \boldsymbol{\alpha}_{21}\boldsymbol{\beta}_{01}\overline{\mathbf{U}}^{n-1}_{1b}\left(\frac{r_0^2}{z}\right)$$

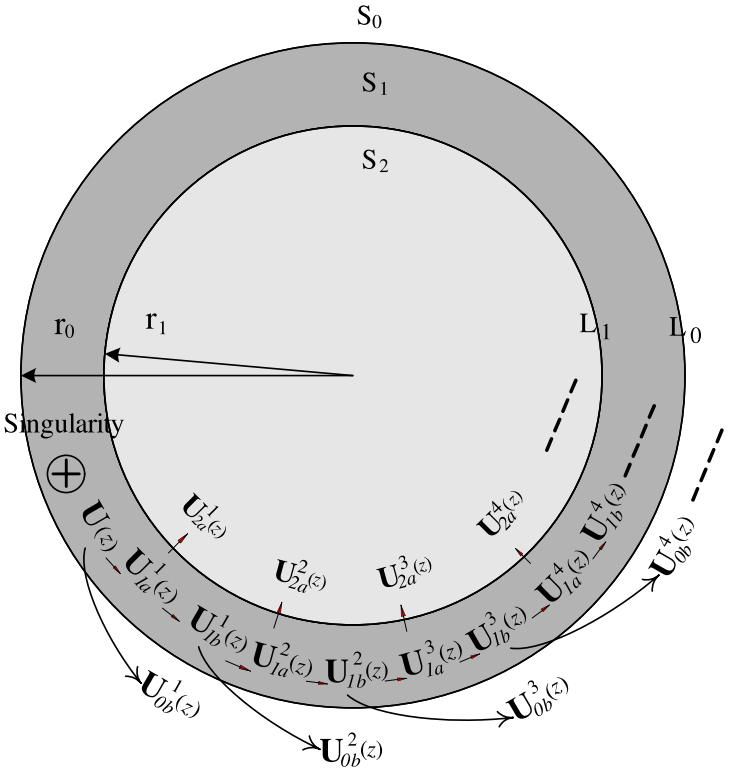

Fig. 7. Procedure for solving the problem of a three-layer composite with a singularity located in the inter-layer.

$$\mathbf{U}_{3a}^{n}(z)=\boldsymbol{\alpha}_{32}\boldsymbol{\beta}_{12}\boldsymbol{\beta}_{32}\mathbf{U}_{2a}^{n-1}\left(\frac{r_2^2}{r_1^2}z\right)+\boldsymbol{\alpha}_{32}\boldsymbol{\alpha}_{21}\boldsymbol{\beta}_{01}\overline{\mathbf{U}}_{1b}^{n-1}\left(\frac{r_0^2}{z}\right)$$

$$\mathbf{U}_{0b}^{n}(z)=\boldsymbol{\alpha}_{01}\mathbf{U}_{1b}^{n-1}(z)$$

$$\mathbf{U}_{1b}^{n}(z)=\boldsymbol{\beta}_{21}\boldsymbol{\beta}_{01}\mathbf{U}_{1b}^{n-1}\left(\frac{r_0^2}{r_1^2}z\right)+\boldsymbol{\alpha}_{12}\boldsymbol{\beta}_{32}\overline{\mathbf{U}}_{2a}^{n-1}\left(\frac{r_2^2}{z}\right)$$

$$\mathbf{U}_{2b}^{n}(z)=\boldsymbol{\beta}_{32}\boldsymbol{\beta}_{12}\boldsymbol{\beta}_{32}\overline{\mathbf{U}}_{2a}^{n-1}\left(\frac{r_2^4}{r_1^2z}\right)+\boldsymbol{\beta}_{32}\boldsymbol{\alpha}_{21}\boldsymbol{\beta}_{01}\mathbf{U}_{1b}^{n-1}\left(\frac{r_0^2}{r_2^2}z\right)$$

4.2.2. A three-layer composite

For the case of three-layer composite with a singularity located in the inter-layer S_1 (Fig. 8), by the same procedures used in the previous section, the solution can be obtained as

$$\begin{cases}\mathbf{U}_0(z)=\mathbf{D}_0\log\left(\frac{z}{r_0}\right)+\mathbf{D}_1\log(r_0)+\boldsymbol{\alpha}_{01}\mathbf{U}^*(z)+\boldsymbol{\alpha}_{01}\boldsymbol{\beta}_{21}\sum_{n=0}^{\infty}(\boldsymbol{\beta}_{01}\boldsymbol{\beta}_{21})^n\left[\overline{\mathbf{U}}\left(\frac{r_1^{2n+1}}{r_0^{2n}}\frac{1}{z}\right)+\boldsymbol{\beta}_{01}\mathbf{U}^*\left(\frac{r_0^{2n+2}}{r_1^{2n+2}}z\right)\right]\\ \mathbf{U}_1(z)=\sum_{n=0}^{\infty}(\boldsymbol{\beta}_{01}\boldsymbol{\beta}_{21})^n\left[\mathbf{U}\left(\frac{r_1^{2n}}{r_0^{2n}}z\right)+\boldsymbol{\beta}_{01}\overline{\mathbf{U}^*}\left(\frac{r_0^{2n+2}}{r_1^{2n}}\frac{1}{z}\right)\right]+\boldsymbol{\beta}_{21}\sum_{n=0}^{\infty}(\boldsymbol{\beta}_{01}\boldsymbol{\beta}_{21})^n\left[\overline{\mathbf{U}}\left(\frac{r_1^{2n+1}}{r_0^{2n}}\frac{1}{z}\right)+\boldsymbol{\beta}_{01}\mathbf{U}^*\left(\frac{r_0^{2n+2}}{r_1^{2n+2}}z\right)\right]\\ \mathbf{U}_2(z)=\boldsymbol{\alpha}_{21}\sum_{n=0}^{\infty}(\boldsymbol{\beta}_{01}\boldsymbol{\beta}_{21})^n\left[\mathbf{U}\left(\frac{r_1^{2n}}{r_0^{2n}}z\right)+\boldsymbol{\beta}_{01}\overline{\mathbf{U}^*}\left(\frac{r_0^{2n+2}}{r_1^{2n}}\frac{1}{z}\right)\right]\end{cases}\tag{21}$$

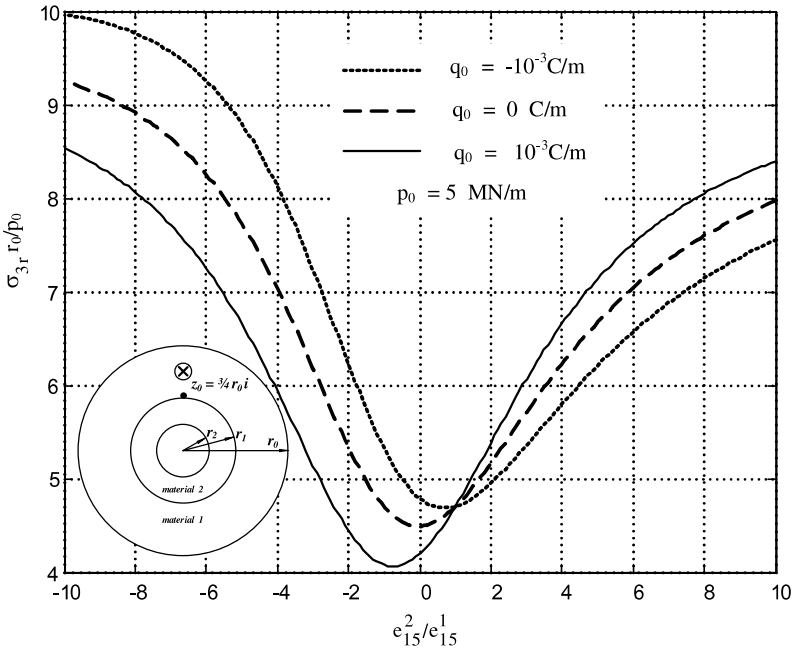

Fig. 8. Distribution of normal stress for different ratio of piezoelectric constants.

5. Results and discussion

Eqs. (7)–(21) give a general series solution of a multilayered piezoelectric composite composed of any number of concentric layers subjected to electromechanical loadings. However, it is relatively valuable to analyze a concentric bimaterial annulus for the sake of practicability. The solution for the current problem can be immediately obtained by substituting $\boldsymbol{\beta}_{01} = \boldsymbol{\beta}_{32} = \mathbf{I}$ into Eq. (20), where $\mathbf{I}$ represents an 2×2 identity matrix. If the radius of each boundary circle keeps $r_2/r_1 = r_1/r_0 = 1/2$, one can obtain

$$\begin{cases} \mathbf{U}_1(z) = \mathbf{U}(z) + \overline{\mathbf{U}^*}\left(\frac{r_0^2}{z}\right) + \sum_{n=1}^{\infty} \boldsymbol{\gamma}_{bn}\left[\mathbf{U}^*(4^n z) + \overline{\mathbf{U}}\left(\frac{r_0^2}{4^n z}\right) + \mathbf{U}\left(\frac{1}{4^n} z\right) + \overline{\mathbf{U}^*}\left(\frac{4^n r_0^2}{z}\right)\right] \\ \mathbf{U}_2(z) = \sum_{n=1}^{\infty} \boldsymbol{\gamma}_{an}\left[\mathbf{U}\left(\frac{1}{4^{n-1}} z\right) + \overline{\mathbf{U}^*}\left(\frac{4^{n-1} r_0^2}{z}\right) + \mathbf{U}^*(4^{n+1} z) + \overline{\mathbf{U}}\left(\frac{r_0^2}{4^{n+1} z}\right)\right] \end{cases} \tag{22}$$

$$\begin{aligned} \boldsymbol{\gamma}_{a1} &= \boldsymbol{\alpha}_{21} \\ \boldsymbol{\gamma}_{b1} &= \boldsymbol{\beta}_{21} \\ \boldsymbol{\gamma}_{an} &= \boldsymbol{\alpha}_{21}\boldsymbol{\gamma}_{b(n-1)} + \boldsymbol{\beta}_{12}\boldsymbol{\gamma}_{a(n-1)} \\ \boldsymbol{\gamma}_{bn} &= \boldsymbol{\alpha}_{12}\boldsymbol{\gamma}_{a(n-1)} + \boldsymbol{\beta}_{21}\boldsymbol{\gamma}_{b(n-1)} \quad \text{for } n > 2 \end{aligned}$$

In the following discussion, the piezoelectric constants of material 1 are assumed as $c_{44}^1 = 35.3\ \mathrm{GN\ m^{-2}}$, $\varepsilon_{11}^1 = 15.1\ \mathrm{nCV^{-1}\ m^{-1}}$, $e_{15}^1 = 10\ \mathrm{C\ m^{-2}}$ and other values are stated specially. Figs. 8 and 9 show the shear stress and electrical field distributions for the bimaterial as function of different ratios of piezoelectric constants, respectively. It is interesting to note that when the piezoelectric constant of each layer are identical, the shear stress cannot be disturbed by the point electrical loading. The maximum normal electric field increases with the decreasing stiffness of the inner material. This phenomenon is helpful for us to design a most sensitive sensor. Figs. 10 and 11 respectively display the angular variations of tangential electric field and

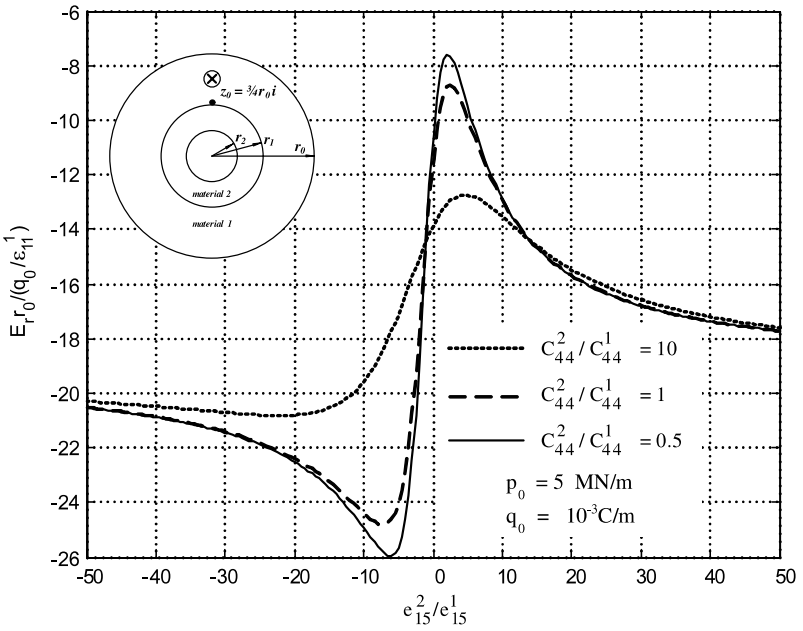

Fig. 9. Distribution of normal electric field for different ratio of piezoelectric constants.

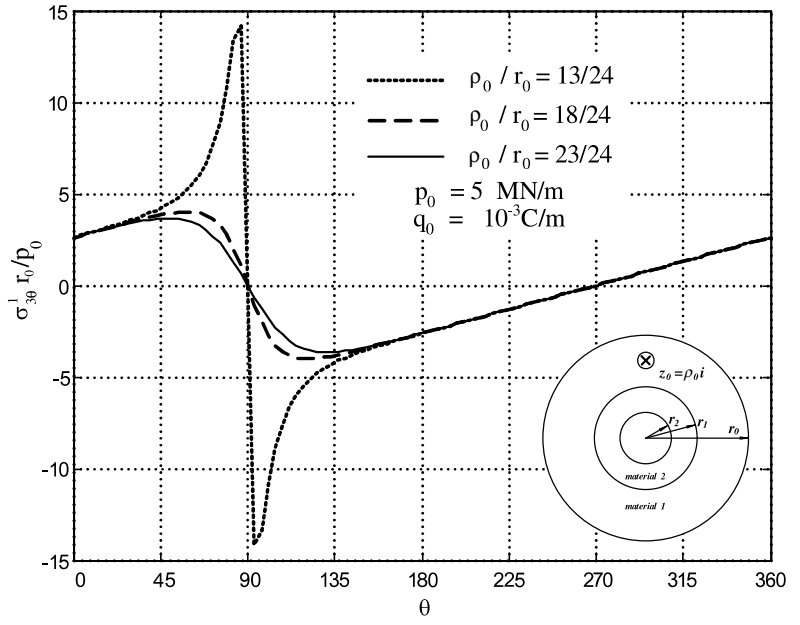

Fig. 10. Angular variations of the interfacial tangential shear stress of the bimaterial concentric annulus.

shear stress along the interfaces of the bimaterial concentric annulus with inner layer being PZT-7A and outer layer being PZT-5H. The material constants of this system are $c_{44}^1 = 35.3\ \mathrm{GN\,m^{-2}}$, $\varepsilon_{11}^1 = 15.1\ \mathrm{nCV^{-1}\,m^{-1}}$, $e_{15}^1 = 17\ \mathrm{C\,m^{-2}}$ and $c_{44}^2 = 25.4\ \mathrm{GN\,m^{-2}}$, $\varepsilon_{11}^2 = 4.071\ \mathrm{nCV^{-1}\,m^{-1}}$, $e_{15}^2 = 9.2\ \mathrm{C\,m^{-2}}$. It is

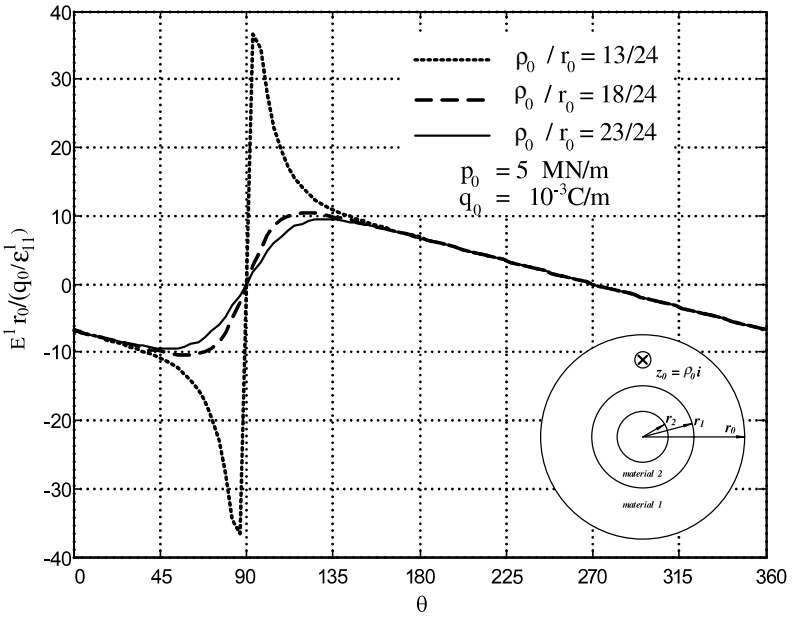

Fig. 11. Angular variations of the interfacial tangential electric field of the bimaterial concentric annulus.

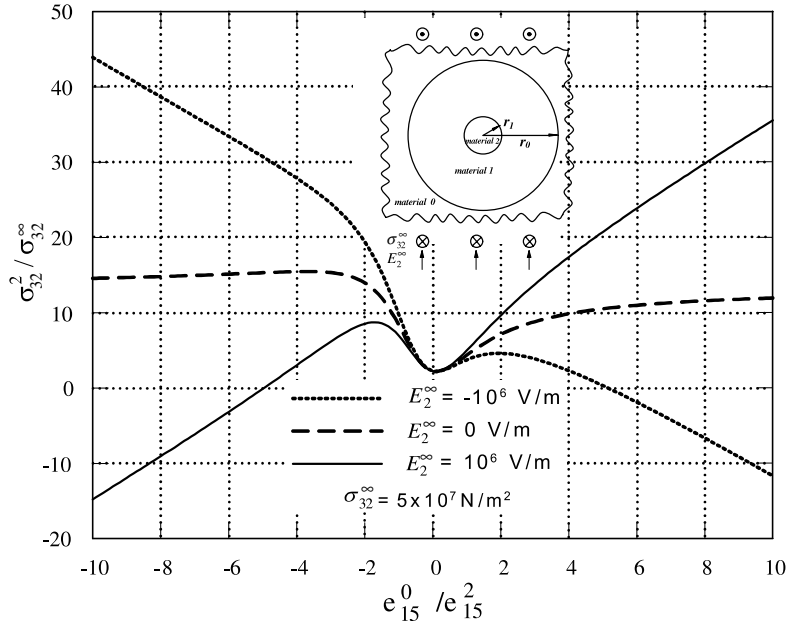

Fig. 12. Stress concentrations as a function of piezoelectric constant ratio. ($c^0_{44} : c^1_{44} : c^2_{44} = 1 : 5 : 10$, $\varepsilon^0_{11} : \varepsilon^1_{11} : \varepsilon^2_{11} = 1 : 5 : 10$, $e^1_{15} = 0.5e^2_{15}$, $r_0/r_1 = 10$).

clear that both the electric field and shear stress experience a jump across the point $\theta = 90°$ when the point loadings approach to the interface. Note that the calculated results of the current problem are obtained from the series solution up to the first 40 terms in Eq. (22) with an error less than 0.05% as compared to a sum of

the first 30 terms. Finally, in order to examine the accuracy of the present derived solution, we consider a three-phase piezoelectric cylinder model subjected to far-field electromechanical loadings. According to Eq. (16), the stress concentrations as a function of piezoelectric constant ratio are shown in Fig. 12. The material constants of the inclusion are assumed as $c_{44}^2 = 35.3\ \mathrm{GN\,m^{-2}}$, $e_{15}^2 = 10\ \mathrm{C\,m^{-2}}$, $\varepsilon_{11}^2 = 15.1\ \mathrm{nCV^{-1}\,m^{-2}}$. It is found that the calculated results agree very well with Jiang and Cheung (2001).

6. Conclusion

The singularities problems in a circularly cylindrical layered piezoelectric media are analyzed in the framework of linear piezoelectricity. Base upon the method of analytical continuation and the alternating technique, the solution of the problems in a series form is derived from the corresponding homogeneous solution. A general series solution for multilayered media with any number of concentric layers subjected to arbitrary singularities is obtained which can be applied to a variety of problems, for example, a single inclusion problem, and a bimaterial concentric annulus etc. It was shown that both the stress and electric field are dependent on the mismatch in the material constants, the location of the singularities and the magnitude of the electromechanical loadings. Some certain piezoelectric constants combination to make the composite perform the largest response of electric field is found and can be used to build a relatively effective sensor in a piezoelectric composite material system.

References

Chao, C.K., Chang, K.J., 1999. Interacting circular inclusions in antiplane piezoelectricity. International Journal of Solids and Structures 36, 3349–3373.

Deng, W., Meguid, S.A., 1999. Analysis of a screw dislocation inside an elliptical inhomogeneity in piezoelectric solids. International Journal of Solids and Structures 36, 1449–1469.

Honein, E., Honein, T., Herrmann, G., 1992a. On two circular inclusions in harmonic problems. Quarterly of Applied Mathematics 3, 479–499.

Honein, E., Honein, T., Herrmann, G., 1992b. Further aspects of the elastic field for two circular inclusions in antiplane elastostatics. Journal of Applied Mechanics 59, 774–779.

Honein, E., Honein, T., Herrmann, G., 1995. On the interaction of two piezoelectric fibers embedded in an intelligent material. Journal of Intelligent Material Systems and Structures 6, 229–236.

Huang, Z., Kuang, Z.B., 2001. Dislocation inside a piezoelectric media with an elliptical inhomogeneity. International Journal of Solids and Structures 38, 8459–8480.

Jiang, C.P., Cheung, Y.K., 2001. An exact solution for the three-phase piezoelectric cylinder model under antiplane shear and its applications to piezoelectric composites. International Journal of Solids and Structures 38, 4777–4796.

Lee, K.Y., Lee, W.G., Pak, Y.E., 2000. Interaction between a semi-infinite crack and a screw dislocation in a piezoelectric material. ASME Journal of Applied Mechanics 67, 165–170.

Liu, J.X., Jiang, Z.Q., Feng, W.J., 2000. On the electro-elastic interaction of piezoelectric screw dislocation with an elliptical inclusion in piezoelectric materials. Applied Mathematics and Mechanics 21, 1185–1190.

Liu, Y.W., Fang, Q.H., Jiang, C.P., 2004. A piezoelectric screw dislocation interacting with an interphase layer between a circular inclusion and the matrix. International Journal of Solids and Structures 41, 3255–3274.

Meguid, S.A., Deng, W., 1998. Electro-elastic interaction between a screw dislocation and elliptical inhomogeneity in piezoelectric materials. International Journal Solids and Structures 35, 1467–1482.

Pak, Y.E., 1992. Circular inclusion problem in anti-plane piezoelectricity. International Journal of Solids and Structures 29, 2403–2419.

Wang, X., Shen, Y.P., 2001. On double circular inclusion problem in antiplane piezoelectricity. International Journal of Solids and Structures 38, 4439–4461.

Weichen, S., 1997. Rigid line inclusions under anti-plane deformation and in-plane electric field in piezoelectric materials. Engineering Fracture Mechanics 56, 265–274.

Zhong, Z., Meguid, S.A., 1997. Interfacial debonding of a circular inhomogeneity in piezoelectric materials. International Journal of Solids and Structures 34, 1965–1984.